Award Number: W81XWH-11-1-0834

TITLE: Biomask: An Advanced Robotic System for the Real-time, Autonomous Monitoring and Treatment of Facial Burns of Wounded Soldiers.

PRINCIPAL INVESTIGATOR: Dr. Eileen Moss Clements

CONTRACTING ORGANIZATION: University of Texas at Arlington
Arlington, Texas 76019-0001

REPORT DATE: April 2013

TYPE OF REPORT: Final

PREPARED FOR: U.S. Army Medical Research and Materiel Command
Fort Detrick, Maryland 21702-5012

REPORT DOCUMENTATION PAGE

Form Approved
OMB No. 0704-0188

1. REPORT DATE	2. REPORT TYPE	3. DATES COVERED
April 2013	Final	29 September 2011 – 31 March 2013

4. TITLE AND SUBTITLE
Biomask: An Advanced Robotic System for the Real-time, Autonomous Monitoring and Treatment of Facial Burns of Wounded Soldiers.

5a. CONTRACT NUMBER
W81XWH-11-1-0834

5b. GRANT NUMBER
W81XWH-11-1-0834

5c. PROGRAM ELEMENT NUMBER

6. AUTHOR(S)
Eileen Moss Clements, Muthu Wijesundara

E-Mail: eclements@uta.edu; muthuw@uta.edu

5d. PROJECT NUMBER

5e. TASK NUMBER

5f. WORK UNIT NUMBER

7. PERFORMING ORGANIZATION NAME(S) AND ADDRESS(ES)
University of Texas at Arlington
Arlington, Texas 76019-0001

8. PERFORMING ORGANIZATION REPORT NUMBER

9. SPONSORING / MONITORING AGENCY NAME(S) AND ADDRESS(ES)
U.S. Army Medical Research and Materiel Command
Fort Detrick, Maryland 21702-5012

10. SPONSOR/MONITOR'S ACRONYM(S)

11. SPONSOR/MONITOR'S REPORT NUMBER(S)

12. DISTRIBUTION / AVAILABILITY STATEMENT
Approved for Public Release; Distribution Unlimited

13. SUPPLEMENTARY NOTES

14. ABSTRACT
The ultimate goal of our research effort is to produce a system called the Biomask, intended for use in facial reconstruction after severe burn or blast injury. The expected outcome of this one-year funding period was to develop modules and systems that can be readily used in animal studies to obtain biological and engineering parameters in order to produce a Biomask. Two types of bioreactors were successfully designed, manufactured and implemented for mice and rabbit wound models. Custom developed portable fluid exchange systems were implemented with bioreactors to perform the fluid delivery and extraction process from mice and rabbit wound models. In addition to the bioreactor systems, a microfluidic-based flexible fluid exchange patch was developed for porcine wound models. A novel design and fabrication process for the fluid exchange patch has been demonstrated. The device integrity during fabrication and operation has been verified using computational simulations and experimental laboratory tests. The fluid exchange patch is currently being applied to porcine wound models and its effectiveness is yet to be established.

15. SUBJECT TERMS
Biomask, burn injury, facial reconstruction, wound-healing, bioreactor, flexible microfluidic, and negative-pressure wound therapy.

16. SECURITY CLASSIFICATION OF: U			17. LIMITATION OF ABSTRACT	18. NUMBER OF PAGES	19a. NAME OF RESPONSIBLE PERSON
a. REPORT	b. ABSTRACT	c. THIS PAGE			USAMRMC
U	U	U	UU	31	19b. TELEPHONE NUMBER *(include area code)*

Table of Contents

1. INTRODUCTION:

a. Research Goals and Efforts

The ultimate goal of our research efforts is to produce a multi-module and multi-functional system called Biomask that interfaces directly with a burn on the face, monitors biological signals, and provides targeted therapy in a closed-loop automated manner. The system is intended for use in facial reconstruction after severe burn or blast injury. The functions include wound bed monitoring and optimization, inflammatory attenuation, and replacement of dermis and hypodermis.

During the one year funding period, the University of Texas at Arlington Research Institute's (UTARI) role was to furnish necessary personnel, expertise, materials, supplies, and laboratories to develop and implement a strategy to design and manufacture a prototype device based on the "biomask" concept for the treatment of full and deep partial thickness facial burns of wounded soldiers; whereby the fields of biology, surgery and engineering are combined to develop an advanced robotic system for the real-time, autonomous monitoring and treatment of facial burns, directing tissue regeneration and restoring form and function to damaged tissues.

As promised by the Statement of work, the specific goals associated with this one year are as follows. The expected outcome of the end of this funding period was to develop modules and systems that can be readily used in animal studies to obtain biological and engineering parameters in order to produce a Biomask.

Goal 1: UTARI shall develop fully functional prototype *bioreactors*, capable of delivering and extracting fluids from the wound from each respective animal model. The device shall be designed for testing in *in vivo* mouse and rabbit models by Dr. Robert Galliano's group at Northwestern University. Multiple iterations or versions of the prototypes are part of the requirement in order to ensure the device works in these models.

Goal2: UTARI shall develop a prototype "patch" device that can: (1) facilitate the application and use of a commercially available, negative pressure vacuum device to the prototype; (2) be made of a material that is conformable to anatomical facial features (such as the nose, chin or area around the eyes); (3) perform fluid exchange (extraction and collection of the fluids during negative pressure therapy and delivery of fluids when negative pressure is off); (5) apply negative pressure wound therapy or fluid exchange to more than one region of the patch independently or to the device as a whole; and (6) be tested in an *in vivo* pig burn model for a wound 6cm in diameter.

As a part of the above goals, UTARI shall *in vitro* test, characterize, and provide proof of concept and feasibility of the prototype devices for the functionality.

b. Background

Soldiers in the Iraq and Afghanistan conflicts often have suffered severe blast injuries and trauma after exposure to improvised explosive devices, incendiary devices, and land mine explosions. Yet because of improved body armor, more of them survive with profound wounds. There are more than twice as many burn wounds, especially in the head-face-neck region, than were seen in previous conflicts [1, 2]. In many cases, warriors have sustained severe facial burns with penetrating injury and comminuted fractures, which result in massive reconstructive challenges for plastic and maxillofacial surgeons, making it extremely difficult to restore functional and aesthetic properties [3]. This proposed research aims to investigate paths to produce an advanced therapeutic system *(i.e.,* Biomask) that clinicians could apply directly on the wound to help facial reconstruction advance to an acceptable outcome. The overall goal is to realize a system that can monitor biological signals, provide targeted therapy in a closed-loop automated manner, and bioengineer the lost tissues and layers of facial skin using different cell types and matrices to produce a reliable, physiologic facial and skin construct to restore functional properties of the face.

The current mortality of combat burns is low; however, burns (regardless of severity) can be incapacitating, disfiguring and painful. Beyond physical complications, burn victims may also experience severe psychological and emotional distress due to scarring and deformity. The methods used in facial reconstruction are often difficult and yield marginal outcome even after 30-40 surgeries. The problem that most surgeons face when trying to reconstruct the damaged facial area is impaired suboptimal healing caused by burn eschar, incomplete debridement, low-quality skin replacement, improper substrate adherence, and systematic inflammation [4]. Even in the best cases, repeated releases, grafts, and transfers of tissues may be required, ultimately yielding only a marginally acceptable outcome. Although facial transplantation is promising, the lifelong concerns of immunosuppression and technical limitations of the method also emphasize the lack of adequate surgical options available to facial burn victims [5].

The research conducted at UTARI in this funded year aimed at providing systems and devices in the Biomask is intended to help monitor and optimize the wound bed, attenuate inflammation, and replace the dermis and hypodermis. The Biomask will be capable of applying negative pressure; delivering cells or other matrices for skin reconstruction; detecting biomarkers and physiological parameters for monitoring healing, inflammation, and the presence of bacteria; and delivering therapeutics to clear bacteria and suppress inflammation and immune response. As such, it should enable accelerated and higher quality facial reconstruction compared to the current state-of-the-art surgeries for complex burns of the face.

c. Biomask

The Biomask system will consist of three main components;

Rigid outer shell: This shell will be built based on a 3D scan of the wound/face and will provide stability and protection to the wound and to the rest of the system (Fig. 1a), and will also house valves needed for fluid distribution.

Conformable microfluidic module : This module will comprise a microfluidic-based flexible inner lining along the inside of the rigid shell, made of a biocompatible material, that provides therapeutic delivery, application of negative pressure, and fluid-extraction capabilities (Fig. 1b).

Sensor module: Sensors will be the key components within the Biomask that accurately monitor conditions and help to determine the treatment.

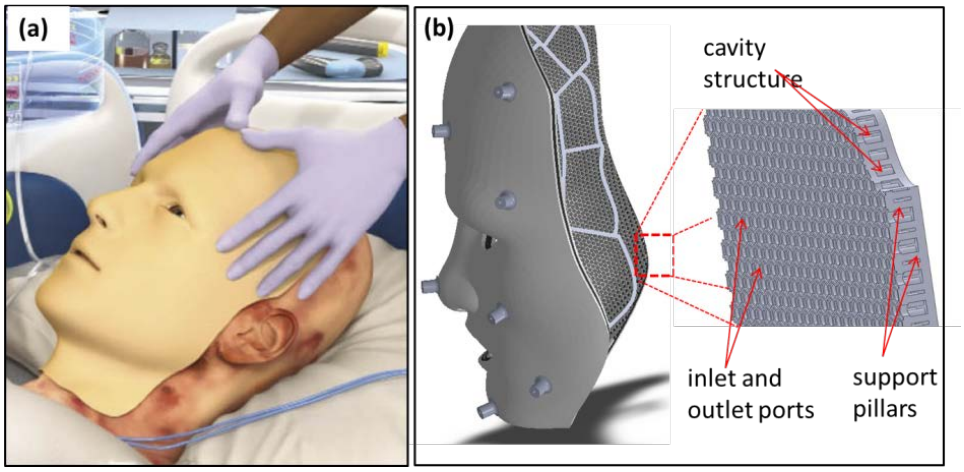

Figure 1: The Biomask system interfaces directly with a burn on the face. (a) The rigid outer shell provides support and protection and (b) The flexible inner lining contains therapeutic delivery and negative pressure capabilities as well as extraction of fluid for analysis

2. BODY

Funding of the Biomask research effort began in September 2011 for a one-year term. One of the main objectives of the long-term collaborative Biomask research is to identify (1) the parameters of the wound-healing process that can be modulated to enable controlled tissue reconstruction and (2) other parameters that are indications of the status of the healing wound. UTARI's and its collaborators' goals were set for initial investigation of the wound healing and tissue regeneration process using animal models. The data obtained in this one year study aims to identify some of the biological parameters of the facial reconstruction process that can be modulated to enable controlled tissue growth and facial restoration. The data would also provide some key engineering specifications for final Biomask productions.

As detailed in goals 1 and 2, our primary objectives during this funding period were to:
(1) Develop novel bioreactor chambers for *in vivo* mouse and rabbit studies monitoring and analyzing wound healing and

(2) Develop novel flexible microfluidic patches for fluid exchange and negative-pressure wound therapy studies on porcine wound models.

Objective 1: Bioreactor System for *in vivo* Mouse and Rabbit Wound Models

UTARI worked with the Northwestern University team to develop custom bioreactor chambers and fluid-exchange systems for their animal studies with mice and rabbits. Throughout the research period, the teams carried out multiple materials and design iterations in order to augment or improve the functionality of the bioreactor. The Northwestern team, under the direction of PI Dr. Robert Galiano, conducted experiments and analyzed the data for this objective.

The key aspect of the bioreactor is its ability to be surgically attached to an animal and utilize the animal body's own vasculature to support the controlled growth of complex tissues. The final design was a three-piece device as shown in Figure 2. Dimensions: 8mm inner diameter, 12mm outer diameter and 8.5mm height. It is composed by a cylindrical base that secures the mouse skin inhibiting epidermal migration and healing by contraction. A mid-section contains two ports with an inner-fenestrated half ring to provide even distribution of perfusates. The base snaps to the mid-section forming the walls of the chamber. Lastly, a clear transparent cap screws to the top of the device. The uniqueness of our chamber is its modularity, which allows to intermittently or continuously deliver agents, such as but not limited to growth factors, nutrients, therapeutics and cells, in order to both enhance tissue growth as well as direct and orchestrate cellular deposition/organization.

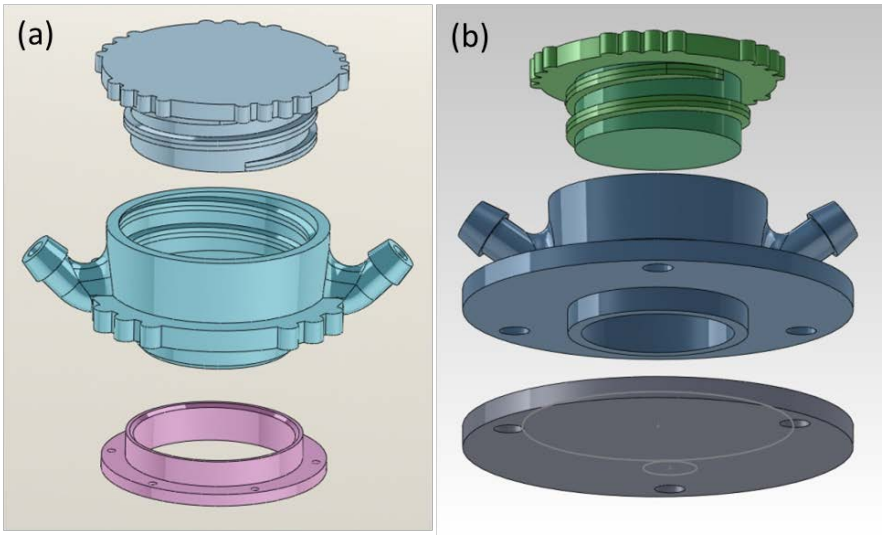

Figure 2: The initial design of the bioreactor for (a) mouse and (b) rabbit wound models

The bioreactor design and development included design, fluidic simulations, manufacturing, and testing (both *in vitro* and *in vivo*). Based on animal studies, multiple iterative development cycles have been performed. In addition, the integration of these bioreactors with externally controlled valves, pumps and custom electronics was also a part of the development process.

Objective 2: Flexible Microfluidic Patches for Porcine Wound Models

UTARI's collaborators at USAISR, located at the Brooke Army Medical Center in San Antonio, TX, under the direction of their PI, Dr. Rodney Chan, are leading the part of the Biomask research involving analyzing skin grafts, the negative pressure effect, and other therapeutic options for restoring tissue on severe burns of the face. Their studies use burn models on the backs of pigs which are 6cm in diameter and range in depth from 1mm to 1cm. The initial fluid-exchange patches developed were tailored for this application. However, as was UTARI's goal, its research of a reliable manufacturing process using a biocompatible silicone-based material resulted in a generic process that allows any size or shaped patch to be made.

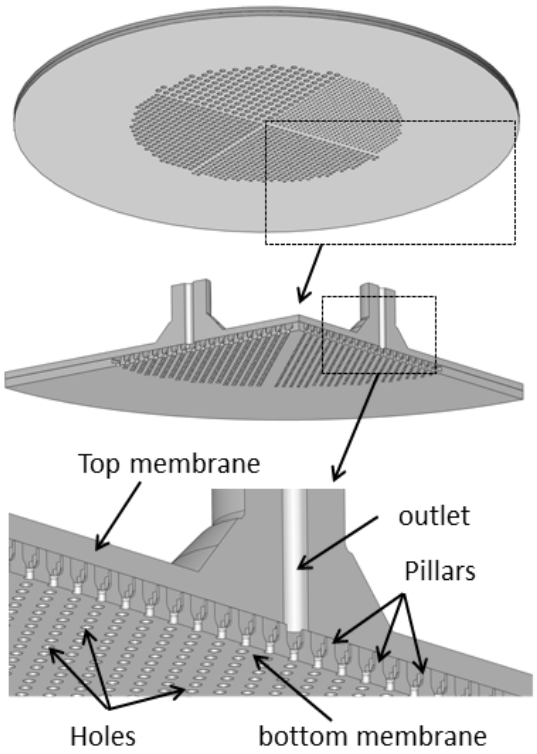

Figure 3: 3D model of the flexible microfluidic patch for fluid exchange.

The objective of this particular research was to develop a flexible patch that could apply negative pressure to the wound as well as perform fluid exchange in a porcine wound model. This work is in line with our ultimate goal of developing a Biomask itself. As described previously, a module of the proposed Biomask consists of a conformable microfluidic layer in a flexible substrate for both monitoring and therapeutic delivery capabilities. Fluid exchange in a flexible patch consists of being able to (1) deliver a fluid to the wound surface and (2) extract whatever fluid is on the surface. The extracting process includes being able to apply negative pressure to the wound. A key aspect of this device is that it should have conformal contact to the wound bed.

The proposed fluid exchange flexible patch consists of a membrane that contacts the wound surface with an array of well-defined microfluidic ports and a cavity structure that facilitates the fluid exchange. Figure 3 shows the design of the microfluidic patch. It is a 9 cm device with four quadrants designed for applying negative pressure and therapeutic delivery on porcine wound models. The device is comprised of: a bottom membrane with distributed inlet/outlet ports that provide direct contact with the wound bed for negative pressure and fluid delivery; cylindrical pillars that support the fluid exchange chamber structure; and a top membrane with inlet/outlet channels that can be connected to fluidic reservoirs and vacuum pumps. The port sizes of each quadrant are 500, 750, 1000, and 1250 µm. The diameter of the pillars is 500 µm and the height is 800 µm. The pillars

are interspaced equally between every grid of four ports, and the gap between pillars also increases as the port size increases, i.e. 750, 1000, 1250, and 1500 µm for the respective port size of 500, 750, 1000, and 1250 µm.

The flexible patch design and development included design, fluidic simulations, manufacturing, and testing (both *in vitro* and *in vivo*). Based on animal studies, multiple iterative development cycles have been performed.

3) KEY RESEARCH ACCOMPLISHMENTS

Objective 1 Accomplishments: Bioreactor chambers and fluid-exchange system for mouse and rabbit studies

Design and manufacturing:

As shown in Fig. 2 (a), the mouse bioreactor chamber consists of three components. The first is a ring that is surgically applied to the wound area on the back of the mouse, while excluding any skin from inside the chamber. The second component is an adapter that slides onto the ring. This adapter contains inlet and outlet ports for fluid exchange as well as an internal microfluidic baffle structure that evenly distributes the fluid entering the chamber. The third component is a cap that is screwed into place inside the adapter. The solid, polished cap allows for clear visualization of the wound surface. The sizes of all the components have been specified for the exact wound size and the desired volume inside the chamber between the bottom of the cap and the wound surface.

The manufacturing process of the bioreactor chambers employs a stereolithography apparatus (SLA), a rapid-prototyping process that can produce high fidelity, complex 3D components. Beginning with a liquid, polymer resin, a laser beam draws out the desired structure and cross-links the polymer layer-by-layer. A variety of SLA resins are commercially available, with varying thermal, mechanical, and chemical resistance properties. Throughout the research period, the teams carried out multiple materials and design iterations in order to augment or improve the functionality of the bioreactor (Figure 4). Testing for mechanical and biocompatible properties led researchers to choose DSM WaterShed XC11122 resin, a material that produces final parts which have good optical clarity after processing and polishing, maintain the necessary mechanical strength throughout use (including sterilization), and are Class IV biocompatible.

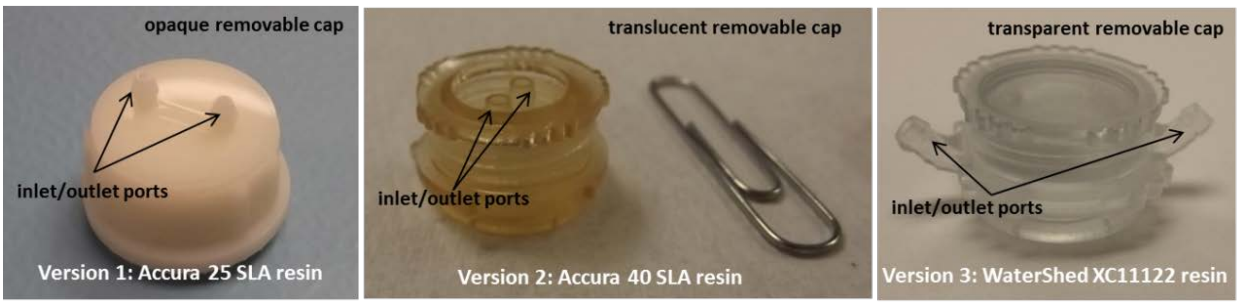

Figure 4: Multiple materials and design iterations of the bioreactor chambers. Version 1: The inlet and outlet ports on the initial bioreactor chamber stuck out from the top of the cap. The material was opaque, and the wound surface could not be visualized. Version 2: The inlet and outlet ports where sunk into the cap for reliability, and the new semi-transparent material allowed some visualization of the wound surface. Version 3: The current bioreactor chamber is made in a clear resin that allows for excellent wound visualization. The inlet and outlet ports now extend from the sides that further increase the visualization as well as provides for an even fluid-flow distribution.

The design improvement and iterative development were based on fluidic simulations, and testing in both *ex situ* and *in vivo* conditions. Fluid should mix well and reach the wound surface during the fluid exchange in order to successfully deliver and remove necessary therapeutics to the wound bed. For optimal fluid delivery ANSYS simulations were carried out to identify the number of fluid channels needed, their respective geometries and flow velocity. Figure 5 shows some representative ANSYS data for (a) number of fluid channels and (b) channel angle.

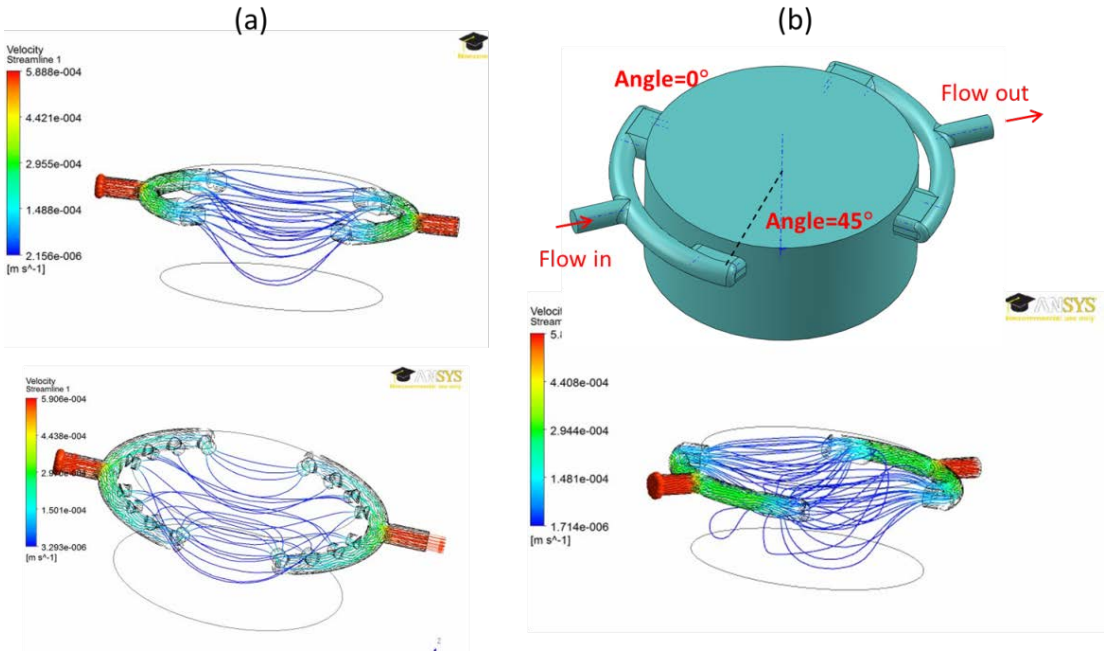

Figure 5: (a) the effect of the number of fluid channels on flow distribution and (b) effect of the channel angle on flow distribution

Similar design and verification pathways have been used for manufacturing rabbit bioreactors. The rabbit bioreactor chamber also consists of three components, but is specifically designed for the rabbit ear. The first component is a solid, flat base that is used on the back side of the ear. The adapter for the rabbit chamber is applied to the top side of the rabbit ear, around the wound, and surgically secured to the ear and the base on the back side. Similar to the mouse bioreactor chamber, the rabbit adapter contains inlet and outlet ports and an internal microfluidic baffle structure. As with the mouse research, the third component is also a solid, polished cap that screws into place inside the adapter. A significant difference between the mouse and rabbit bioreactor chambers was the addition of silicone gaskets attached to the base and adapter for the

rabbit. Due to the natural rigidity and curvature of the rabbit ear, using flat structures could have led to leakage of fluid from inside the chamber. The silicone gaskets added conformity to the chamber, thereby eliminating leakage. These gaskets were made of a liquid silicone that had been molded and cured to specific dimensions. Figure 6 shows the components of the rabbit bioreactor.

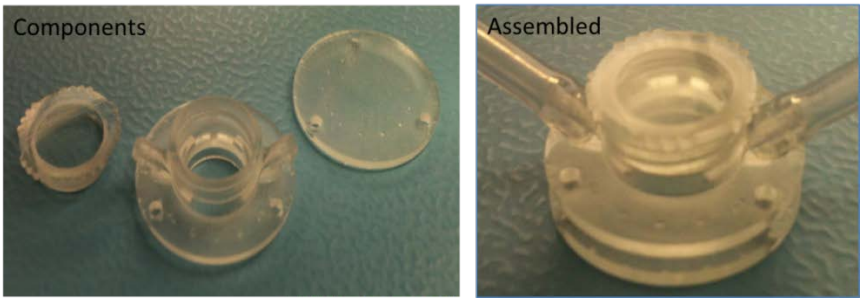

Figure 6: the rabbit bioreactor

System integration:

Two different custom, portable fluid-exchange systems were also developed for use with the mice and the rabbits. Both systems were designed to allow the researcher to set a pre-determined flow rate for the fluid-exchange process. The mouse system is a stand-alone device that connects to the bioreactor chamber on the back of the mouse during the experiment (Figure 7 (a)). In-line y-connectors are used at the outlet of the bioreactor chamber for controlled collection of wound exudate prior to initiating fluid exchange. After the experiment, the system is disconnected from the chamber and silicone plugs are inserted into the inlet and outlet to avoid fluid loss. This system can be used on multiple mice in series. For the rabbit, a self-contained system was developed that allowed it to be secured to the rabbit throughout the duration of the experiment, which could be greater than 40 days (Figure 7 (b)). This allowed for the fluid within the chamber to be continuously exchanged without having to anesthetize and secure the rabbit. A custom jacket was designed with pockets for all the components of the fluid-exchange system: source and waste fluid reservoirs, lightweight pumps and valves, custom-designed electronics, user control interface, and batteries. The system was designed to work with two bioreactor chambers at one time, thereby allowing a chamber to be applied to each ear.

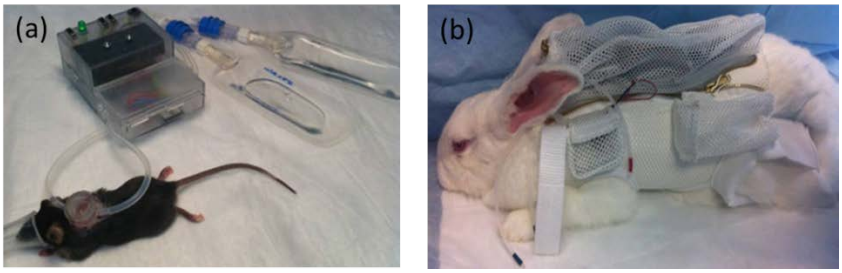

Figure 7: (a) Custom fluid exchange system developed for mice studies and (b) Custom fluid exchange system developed for rabbit studies. The jacket holds all components and can allow autonomous operation for over 24 hours.

In Vivo testing:

One of the main objectives of the long-term collaborative Biomask research is to identify (1) parameters of the wound-healing process that can be modulated to enable controlled tissue reconstruction and (2) other parameters that are indications of the status of the healing wound. UTARI's collaborators at Northwestern University, under the direction of PI Dr. Robert Galiano, conducted experiments and analyzed the data for this objective. Figure 8 shows the two different chambers surgically attached to the wounds on each animal.

Figure 8: Custom-developed bioreactor chambers surgically attached to the back of a mouse (left) and to the ear of a rabbit (right).

Using these bioreactor chambers and fluid-exchange systems, collaborators at Northwestern were able to run initial experiments and collect data on the wound environment during healing. The work is continuing. The current work and future efforts using these bioreactors will be used to guide the research and development of the Biomask for human applications.

Objective 2 Accomplishments: Flexible Microfluidic Patches for Porcine Wound Models

Design and manufacturing:

Figure 9 shows a flexible fluid-exchange patch fabricated at UTARI that can be used on a 6cm diameter burn wound in the pig studies along with a schematic image of the cross-section. The cavity within the patch allows fluid to be distributed throughout the patch so that even delivery occurs at each of the outlet ports along the bottom.

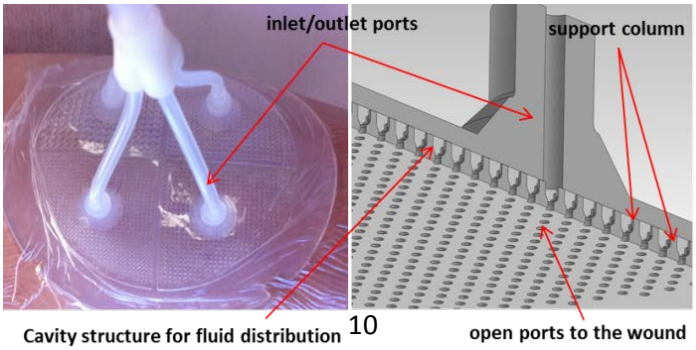

Figure 9: A fluid-exchange module prepared for use on burn wounds in a pig study (left). Schematic cross-section of the fluid-exchange patch showing the fluid cavity, support structures, and ports (right).

Finite element analysis was carried out to test the performance and structural integrity of the device. Material properties used for simulations are presented in Table 1. Due to the symmetry of the device, only one quadrant of the device was simulated. ANSYS simulation was performed to check the structural integrity of the microfluidic chamber as well as to understand the fluid flow characteristics of the device. A negative pressure of 120-140mmHg was applied, which is similar to vacuum levels that are applied in NPWT.

Table 1: Material properties of RTV-4234-T4 after cured with the ratio of 10:1 base to curing agent [6].

Material Property	Value
Tensile Strength	6.7 MPa
Elongation at Break	400 %
Specific Gravity	0.96
Poisson's Ratio	0.48
Young's Modulus	1.675 MPa

Representative data on ANSYS simulation is shown in Figure 9. With the designed dimensions, analysis confirmed that under expected loads (120-140mmHg of negative pressure), the cavity would remain open and support structures would not collapse. The maximum deflection is around 100 µm, which occurs near the outlet of the top membrane; however, the 100 µm deflection should not cause structural problems as the pillar height is 800 µm.

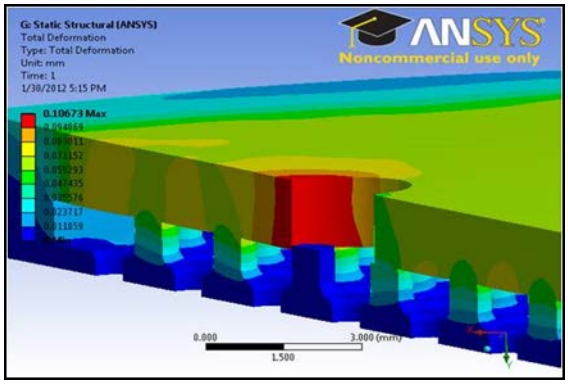

Figure 9: Structural simulation of the fluid-exchange module, showing minimum deflection (during applied negative pressure) which indicates sufficient dimensions and spacing of the supports and ports.

A flow analysis using ANSYS was performed to determine if the current patch design allowed for uniform flow through the device. As an illustration, figure 10 shows the ANSYS computed streamlines for the flow through one quarter of the device. The flow paths indicate a fairly uniform flow characteristic throughout the chamber. We have quantified the uniformity; two inlet flow rates were investigated to see their effect on the outlet flow rates. The results are given in Table 2. The flow mass injected from the inlet is conserved. For the flow of 1.0 ml/minute, the flow rate at outlet 1 is 13.57% and 13.25% higher than that of outlet 2 and 3, respectively. When the flow rate is increased to 5.0 ml/min, the difference of the flow rate of outlet 1 has decreased slightly to 12.83% and 12.29% higher than that of outlet 2 and 3, respectively. Better inlet and outlet placement can mitigate the flow rate differences and further flow optimization can be achieved.

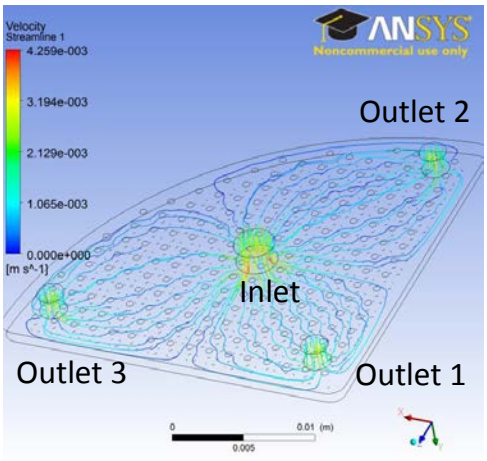

Figure 10: ANSYS simulation results on fluid flow of 1.0ml/min.

Table 2: ANSYS computed flow rates at inlet and outlet channels

Inlet (ml/min)	Outlet 1 (ml/min)	Outlet 2 (ml/min)	Outlet 3 (ml/min)
1.000	0.36186	0.31862	0.31952
5.000	1.768	1.567	1.573

Researchers initially investigated multiple materials, and found that two silicone materials had the desired mechanical characteristics and could be processed into patches as needed. The first material is T4, a silicone from Dow Corning USA, and the second is P20, a silicone from Silicones, Inc. With either material, the key challenges that the project team encountered in developing this process included: the small dimensions of many of the features; obtaining a cured silicone without air bubbles or defects; reliably bonding the silicone layers together, so that they accurately align and will not delaminate, and creating embedded interconnects for connecting external tubing

A two layer molding process was developed for the manufacturing of flexible fluid exchange patch. Figure 11 represent the process flow for making a single patch. The main steps are: (1) create two molds, (2) mold liquid silicone into the molds, (3) release the silicone layers, and (4) bond them together into a single patch.

.

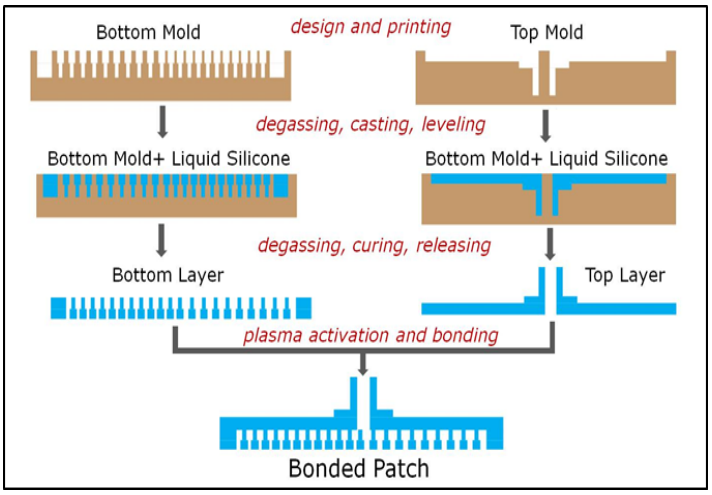

Figure 11: Process flow for manufacturing a fluid-exchange module.

UTARI successfully completed the initial development process and conducted laboratory tests to investigate the reliability of the device during operation and sterilization. Currently, UTARI has a process for manufacturing reliable fluid-exchange patches with varying dimensions for animal studies. Results on each step of the fabrication process are shown in Figure 12.

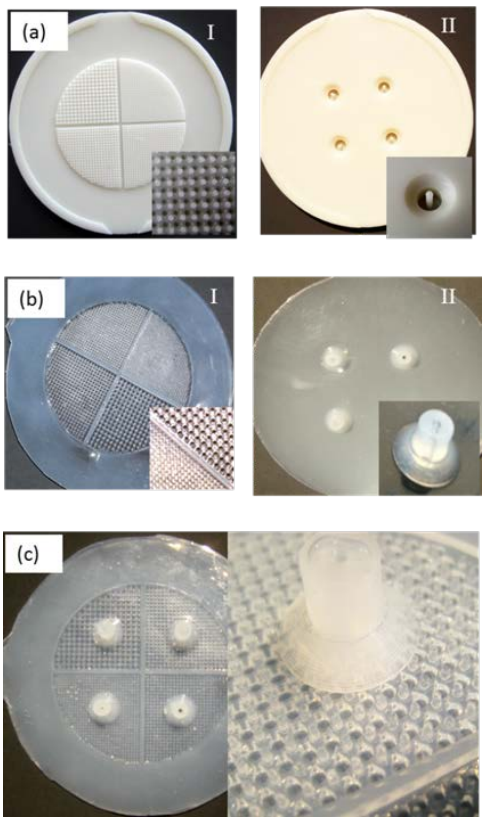

Figure 12: Various stages of two-layer fabrication process (a)(I) bottom mold, (a)(II) top mold, (b)(I) bottom membrane (c)(II) top membrane and (c) fabricated patch

Operational characteristics of the device tested on a bench top setting for fluid extraction and delivery using the test setup are shown in Figure 13. In accordance to sterilization and biological media testing that most biomedical devices undergo, the fabricated device was soaked in ethanol as well as subjected to UV radiation for an extended amount of time (12-24 hours). Devices were checked for reliability after exposing to these conditions and no changes to the device integrity were observed.

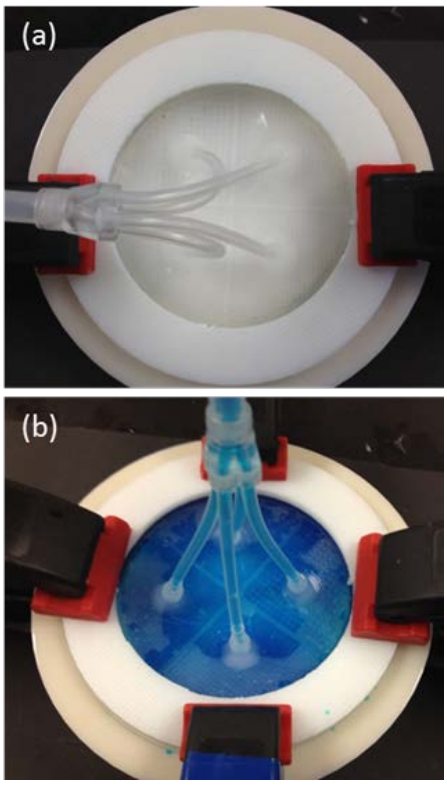

Figure 13: Test set up for fluid extraction and delivery (a) before fluid introduction and (b) after fluid introduction

Within the first six months of the initial funding period, UTARI delivered to USAISR ten identical patches, each with external tubing attached, ready for use in USAISR's animal studies. By nine months, UTARI had another ten patches with a different design delivered to USAISR. Figure 14 shows the flexible fluid exchange patch attached to a wound on a pig. A Journal article detailing the research and analysis on a reliable material and manufacturing process for flexible microfluidic systems has been submitted to The Journal of Micromechanics and Microengineering (see appendix). The feedback from the initial studies at USAISR will guide the designs for the next versions of the fluid-exchange patch for highly contoured surfaces. As of today, UTARI intends to add an adhesive-free attaching capability to the fluid patch; this feature would be highly desirable for the patch for the porcine studies and also in the final human Biomask.

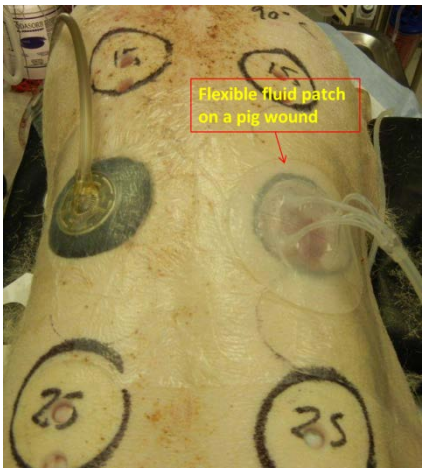

Figure 14: flexible fluid exchange patch attached to a wound on a pig

In addition to flexible fluid exchange patch to porcine wound models, UTARI is currently investigating the manufacturing process for a microfluidic-based flexible fluid-exchange module to perform fluid delivery and extraction, control wound environment, and apply negative-pressure on complex contour surfaces such as the face. The initial results on this effort are depicted in Figure 15.

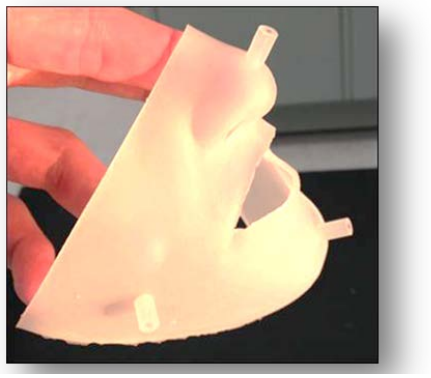

Figure 15: initial fabrication results of a highly contoured fluid exchange patch fabricated using silicone

3. REPORTABLE OUTCOMES

Objective 1 outcomes: Bioreactor chambers and fluid-exchange system for mouse and rabbit studies

1. A reliable manufacturing process has been established to fabricate bioreactors for two animal models (mouse and rabbit)
2. Portable fluid-exchange systems consisting of custom control electronics, pumps, and valves were developed for use with the mice and the rabbits. Both systems allow the researcher to set a pre-determined flow rate for the fluid delivery and extraction process.

3. Prototype systems have been successfully implemented on both mouse and rabbit wound models and the viability of the system for animal studies has been demonstrated.
4. Further *in-vivo* studies using these bioreactor chambers and fluid-exchange systems are continuing at Northwestern University and our collaborators are collecting data on the wound healing parameters.

Objective 2 outcomes: Flexible Microfluidic Patches for Porcine Wound Models

1. A reliable two layer molding process has been established to fabricate flexible fluid exchange patches for porcine wound models
2. Extension of the two layer molding process for fabricating flexible fluid exchange systems for highly contoured surfaces is in progress
3. Prototype patches have been implemented on porcine wound models.
4. *In-vivo* studies using these flexible fluid exchange patches continue at US Army Institute of Surgical Research.

4. CONCLUSIONS

With regards to objective 1, mouse and rabbit bioreactors were successfully designed, manufactured and implemented. Both types of chamber bioreactors consist of three main components, but the design has changed from the mouse to the rabbit bioreactor. Due to the natural rigidity and curvature of the rabbit ear, implementing the rabbit bioreactor was challenging, however, using an extra component, a custom silicone gasket, difficulties caused by fluid leakage was mitigated. In addition to bioreactors, custom developed portable fluid-exchange systems were successfully demonstrated. These systems along with bioreactors allow researchers to perform the fluid delivery and extraction process from mouse and rabbit wound models with precise control.

With regards to objective 2, the design and fabrication of a flexible microfluidic-based fluid exchange patch using a two-layer molding process has been demonstrated. The device integrity during fabrication and operation has been verified using computational simulations and experimental laboratory tests. The device is capable of delivering and extracting fluid to and from a wound site. The fluid exchange patch is currently being applied to porcine wound models and its effectiveness is yet to be established. Further device iterations are expected for deep wounds as well as wounds with complex topographies.

5. REFERENCES

1. D. S. Kauvar, *et al.*, "Burns sustained in combat explosions in Operations Iraqi and Enduring Freedom (OIF/OEF explosion burns)," *Burns*, vol. 32, pp. 853-857, Nov 2006.
2. J. Geiling, *et al.*, "Medical Costs of War in 2035: Long-Term Care Challenges for Veterans of Iraq and Afghanistan." *Military Medicine*, vol 177(11) pp.1235-1244, Nov 2012
3. C.H. Thorne, *et al.*, eds. *Grabb and Smith's Plastic Surgery*, 6th ed.: Lippincott Williams & Wilkins, 2006.
4. R.G. Hale, *et al*. Maxillofacial and Neck Trauma, Chapter 6, *Combat Casualty Care* 2012 (http://www.cs.amedd.army.mil/borden/book/ccc/UCLAchp6.pdf)
5. C.R. Gordon *et al.*, The world's experience with facial transplantation: what have we learned thus far? *Ann Plast Surg* vol 63, pp572-578. 2009
6. https://www.xiameter.com

APPENDIX 1:

Manuscript submitted for Journal Publication

Fabrication of Compliant Silicone Microfluidics for Biomedical Applications

Muthu B.J. Wijesundara[1], Sean Collignon[1], Raminderdeep Sidhu[1], Jeongsik Sin[1], Shrinivas Apte[2], Ashkan Akbariyeh[2], Brian H. Dennis[2], Eileen Moss Clements[1]
[1]University of Texas at Arlington Research Institute, the University of Texas at Arlington, Texas, USA
[2]Department of Mechanical & Aerospace Engineering, the University of Texas at Arlington, Texas, USA
E mail: muthuw@uta.edu

Abstract:

Microfluidics on compliant substrates has become increasingly significant in clinical applications that include gene manipulation, drug delivery, toxin and pathogen detection, point-of-care diagnostics, and tissue engineering. The work detailed in this paper outlines the design and fabrication aspects of clinically relevant flexible microfluidic devices including material selection, verification of fabrication steps, evaluating bond strength between layers, and testing structural integrity during operation. A microfluidic device that is intended to study wound healing process parameters is used for highlighting critical design and process aspects. The functions of this particular device include applying negative pressure wound therapy and delivering therapeutics to a wound. Silicone RTV-4234-T4™ was used because of its desired chemical and mechanical properties that include biocompatibility, chemical inertness, extreme flexibility, and high tear strength. A two layer molding process followed by plasma activated bonding was employed to create the device. Numerical simulations and *in vitro* testing were conducted for verifying the device integrity during fabrication and operation. The bond strength between two layers exceeds 100kPa and the device endures operational and sterilization conditions.

Key words: compliant, silicone, microfluidics, RTV-4234-T4, NPW

1. Introduction:

Microfluidics has impacted many scientific and technological fields from chemistry to biology to engineering. This technology offers novel capabilities for biomedical applications that include gene manipulation and analysis, drug development and delivery, toxin and pathogen detection, point-of-care diagnostics, and tissue engineering [1]. Microfluidic devices and systems are typically made using rigid substrates, flexible substrates, or a combination of both. However, many emerging areas in biomedical applications require microfluidics on flexible, biocompatible substrates, due to the necessity of conformal contact of the device to the applied part of the body or organs. Examples include implantable health monitors, drug delivery systems, wound healing and management systems, and prosthetics [2-6]. In order to fully serve these vital application areas, more research and development is needed for fabricating microfluidic platforms out of highly flexible biocompatible substrates.

Organic polymers are typically the leading materials for compliant microfluidic devices, systems, and parts because many of them offer desired biocompatibility and flexibility [7, 8]. For instance, a *polydimethylsiloxane* (PDMS) based flexible microfluidic wound dressing device has been successfully implemented to induce tissue microdeformation on wounds [4]. A polymer microfluidic bandage that can diffuse oxygen to the wound bed has shown to offer insight into the oxygen-enhanced wound healing process [5]. Ziegler et al. has reported the fabrication and testing of a parylene based device with an array of neural probes containing fluidic channels that are capable of delivering small amounts of drugs into biological tissue and performing neural recording [9]. A recent report shows the differentiation of embryonic stem cells into cardiomyocytes in a compliant microfluidic system [10]. Considering the wide array of available organic polymers that provide the desired flexibility and biocompatibility, the selection of a specific polymer or set of polymers is typically governed by the device function, applied environment, and fabrication methodology.

To date, silicones have become the materials of choice in fabricating microfluidics for biomedical applications. Among many other silicones, PDMS has become the primary material for rapid prototyping of complex microfluidic systems because of its simple manufacturing process and highly consistent results [11, 12]. Despite the wide spread usage and success in the fabrication of many microfluidic devices, PDMS has its own limitations as a universal material for biomedical microfluidic applications [13]. For instance, PDMS is permeable to many gases and small molecules. Although this is advantageous toward applications including cell culture, gas separation membranes, and soft-lithography, the same property can lead to adverse effects when applied to analytical devices or drug delivery applications. PDMS has also been shown to absorb organic and biological molecules including testosterone and androstenedione, limiting its applications in drug delivery [8, 14]. Solutions to alter permeability have been attempted by changing the mixing ratio of the base and curing agent, or coating PDMS with other materials, however, this increases the rigidity of the material, limiting compliant functionality [15, 16]. These shortcomings restrict implementation of PDMS-based microfluidics from many clinically relevant biomedical applications. Therefore, it is important to investigate other polymers, particularly other flexible silicones for compliant microfluidic platforms.

Understanding the relationship between the application requirements and material properties is crucial during polymer material selection. In addition to the biochemical behavior of materials, other physical properties such as tear strength, tensile strength, percent elongation, and hardness are critical factors. For example, the tear strength of a material is very critical when a thin layer of it is used in wound dressings and implantable devices [17]. The removing or replacing of these devices from soft tissues after usage can be very tricky if the material has a very low tear resistance. Additionally, the hardness and percent elongation are critical for both operational and manufacturing aspects of the microfluidic components. Finally, flexibility must be taken into consideration when the device is made for

implantable, wearable, or wound dressing applications.

Methodologies applied in the fabrication of polymer microfluidics include: conventional lithography based fabrication; replica molding or casting; and injection molding [18]. Among them, replica molding using prefabricated molds or stamps is widely popular because of the simplicity of the method, yet it is capable of creating complex geometries. The fabrication process developed in this work will also use replica molding to create compliant microfluidic systems. The process starts by casting thermal or UV curable polymer onto a prefabricated mold. Once the liquid polymer conforms to the shape of the features on the master, the polymer is cured and subsequently peeled off from the master creating a negative replica of the mold. Then the replica is bonded to a substrate made of either a similar or different material to create microfluidic channels. Replica molding has been used for creating many microfluidic devices with feature sizes varying from micro to nanometer scales [19, 20, 21]. Once the master mold is created, replication does not require expensive equipment and cleanroom conditions; therefore, this method is widely accepted in research and development environments [11].

Regardless of which fabrication route is taken or what kind of architecture is selected, one of the vital aspects of microfluidic device fabrication is the requirement of a bonding process to create enclosed microstructures. In addition to the importance of providing structural integrity, the bond must prevent leakage and should not interfere with device functionality. Bonding methods used in microfluidic fabrication can be categorized into two major techniques: applying auxiliary materials such as adhesives and solvents, and surface activated bonding [22]. In many cases, surface activated bonding methods are preferred because auxiliary materials may interfere with device functionality in terms of material compatibility and/or altering the geometrical features of the fluidic structure. For silicone fabrications, oxygen plasma assisted bonding is widely used because of its suitability for the material. Even though PDMS-PDMS and PDMS-glass are the most investigated silicone systems, extending this knowledge to other types of silicone materials is relatively simple.

The work presented here details the fabrication and testing of a microfluidic device that is intended for studying the parameters that affect the wound healing process including micro deformation of the wound bed due to negative pressure wound therapy (NPWT). Based on its material properties, the silicone RTV-4234-T4 was selected as the primary material and the device was generated using a dual layer fabrication process. Experiments and results discussed here highlight material characteristics, fabrication issues, and operational aspects with respect to this particular device and its applications. Nonetheless, processes and analyses described are generic and applicable to the fabrication of any compliant silicone microfluidic device.

2. **Experimental:**

2.1. *Design and Simulations*

The device is a 9 cm round patch with four quadrants designed for applying NPWT and therapeutic delivery on porcine wound models. The device (figure 1) is comprised of: a bottom membrane with distributed inlet/outlet ports that provide direct contact with the wound bed for NWPT and fluid delivery; cylindrical pillars that support the fluid exchange chamber structure; and a top membrane with inlet/outlet channels that can be connected to fluidic reservoirs and vacuum pumps. The port sizes of each quadrant are 500, 750, 1000, and 1250 µm. The diameter of the pillars is 500 µm and the height is 800 µm. The pillars are interspaced equally between every grid of four ports, and the gap between pillars also increases as the port size increases, i.e. 750, 1000, 1250, and 1500 µm for the respective port size of 500, 750, 1000, and 1250 µm.

Finite element analysis was carried out to test the performance and structural integrity of the device. Material properties used for simulations are presented in Table 1. Due to the symmetry of the device, only one quadrant of the device was simulated. ANSYS

simulation was performed to check the structural integrity of the microfluidic chamber as well as to understand the fluid flow characteristics of the device. For the negative pressure applications, the bottom membrane is fixed thereby allowing the top portion to displace due to the negative pressure acting on the inside walls. To satisfy symmetry conditions, deformation normal to symmetry surfaces was also fixed. A negative pressure of 18.6 kPa was applied, which is similar to vacuum levels that are applied in NPWT. For the flow simulation, the geometry of the device consists of three parts, the top, the bottom, and the supports (pillars) in-between. Two flow rates were studied, 1 and 5 ml/min.

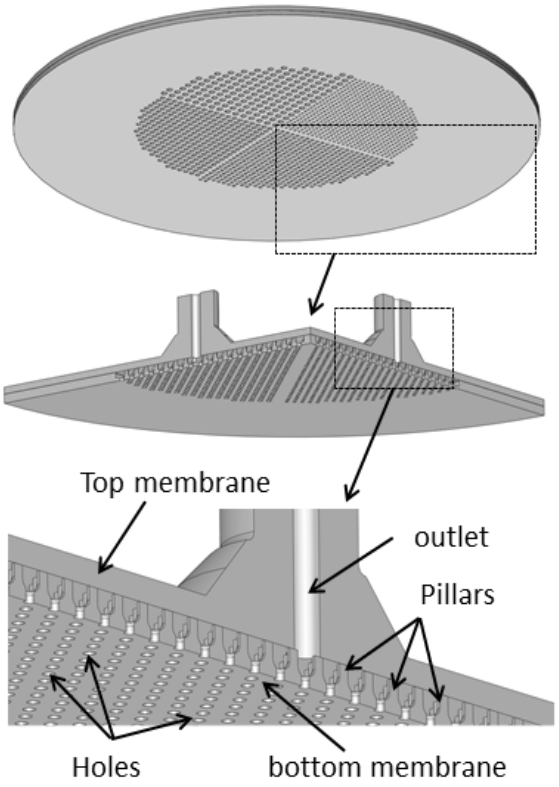

Figure 1: Schematic representation of the microfluidic device design for wound healing studies, insets show the close-us with cross-sectional view.

Table 1: Material properties of RTV-4234-T4 after cured with the ratio of 10:1 base to curing agent [23].

Material Property	Value
Tensile Strength	6.7 MPa
Elongation at Break	400 %
Specific Gravity	0.96
Poisson's Ratio	0.48
Young's Modulus	1.675 MPa

COMSOL was used to validate the structural integrity during the pressure induced bonding process. In the plasma activated bonding process, activated surfaces of two membranes were pressed against each other at 20 kPa. In the simulation, the bottom membrane was fixed to a stationary solid chuck and the top membrane was on a movable solid chuck that applies pressure to the top of the two membranes.

2.2. Fabrication (Molding and Bonding)

Figure 2 shows the two layer fabrication process flow of a compliant microfluidic device. All molds were generated on Accura 25 resin using a 3D Resin Printing System (Viper SLA®, **3D Systems Corporation**). **Molds were then coated with 3µm of parylene to reduce the stiction of the silicone materials to the mold. The silicone material used for the molding process was** RTV-4234-T4 (XIAMETER from Dow Corning). RTV-4234-T4 is a two component (base and curing agent) thermal curing material system similar to commonly used PDMS. In a typical process, the base material was mixed with the curing agent at a 10:1 ratio; however, the molding process used here adds a third component (99% anhydrous hexane, Sigma Aldrich) in order to reduce the viscosity. This is vital for microscale molding as high viscosity materials have difficulty flowing into microscale features on the mold. In the final mixture, the base material to hexane to curing agent ratio was 10:10:1. The base material was first mixed with hexane for an hour before mixing with the curing agent. The mixture was degassed for 15 minutes at 100 torr before spreading and leveling on the mold. Once the silicone mixture was applied and leveled, the silicone was cured at 62°C for 30 minutes.

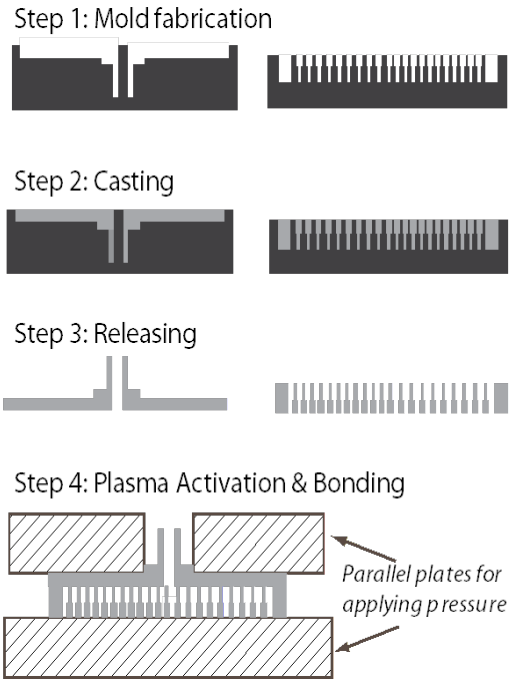

Figure 2: Two layer fabrication process flow of a compliant microfluidic device with a chamber for fluid exchange

Released membranes were then exposed to oxygen plasma (4% oxygen in argon) for 20 seconds at 200 watts and 150 mtorr in a March PX 250 Plasma Reactor. Activated surfaces were then manually pressed against each other using two parallel aluminum plates. The two membranes were further pressed for 10 minutes using a Laurier M-9A Flip-chip bonder at 10,000 grams of force and 75°C temperature to eliminate any unbonded areas due to surface defects. One critical factor in a two-layer bonding process is the alignment. In this case, pillars and ports must be perfectly aligned to each other. To address this issue in design, pillars and ports were created together on the bottom membrane so that no further alignment is required during the bonding process. Furthermore, inlets and outlets of the top membrane should accurately position on the chamber structure to achieve proper vacuum and fluid distribution characteristics. This was achieved through alignment features.

2.3. *Testing*

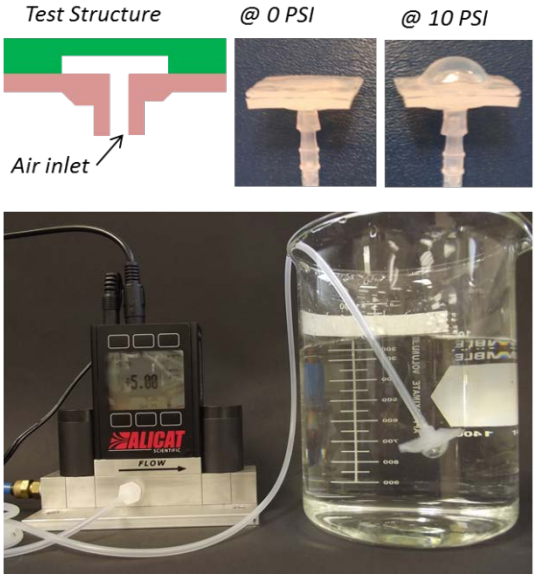

Figure 3: (a) The test structure and (b) the test setup used in the delamination test

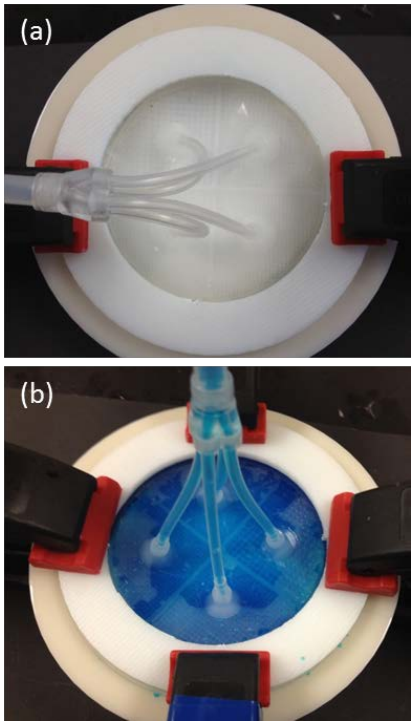

Figure 4: Test set up for fluid extraction and delivery (a) before fluid introduction and (b) after fluid introduction

Structural integrity of the RTV-4234-T4 silicone and the bonding were tested using a structure shown in figure 3. Regulated air pressure was introduced into the chamber structure with increments of 1 psi at time intervals of 5s until the material or bond integrity was compromised. Both visual inspection and bubble formation in a water bath were used to record the maximum pressure needed for rupture or delamination. Operational characteristics of the device tested for fluid extraction and delivery using the test setup shown in figure 4. In accordance to sterilization and biological media testing that most biomedical devices undergo, the fabricated device was soaked in ethanol as well as subjected to UV radiation for an extended amount of time (12-24 hours). Devices were checked for reliability post exposure.

3. Results and Discussion:

3.1 Design and Simulation

The microfluidic device presented here is intended for identifying the parameters of the wound healing process that can be modulated to enable controlled tissue growth. The basic functions of the device are applying NPWT, delivering therapeutics to the wound surface and removing exudate from the wound. A detailed description of the device with four distinct quadrants is given in the experimental section. Each quadrant consists of one inlet and three outlets (see fluidic simulation section for the placement of outlets). The ports on the bottom layer that are in direct contact with the wound bed differ in size from quadrant to quadrant. Researchers have hypothesized that microdeformation due to NPWT promotes cell proliferation and helps wound healing [24]. A recent study also confirmed that microfluidic membranes with different port sizes can be used to alter the microdeformation of the wound beds [4]. This particular device would be able to quantitatively analyze the size scale effect of microdeformation on wound healing because the four quadrant approach eliminate wound-to-wound variations due to physiological and experimental variations.

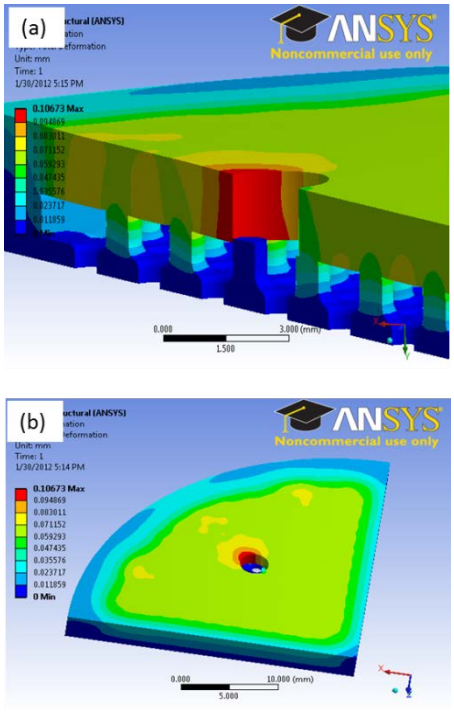

Figure 5: (a) ANSYS simulation results on a cross-section showing the stress under negative pressure of 18.6 kPa (b) ANSYS simulation results showing the stress distribution on the top membrane under negative pressure of 18.6 kPa.

With one of the functions being the application of NPWT, the chamber should not collapse under applied negative pressure conditions. The determining design factors are the geometry and the gap between the supporting pillars. The simulations were performed for the gap of 1500 µm with pillar geometry of 500 µm in diameter and 800 µm in height. Wider gap conditions were tested in simulations as they would result in the maximum possible deflection. The applied negative pressure was 18.6 kPa, a typical value for NPWT. Figure 5(a) depicts the cross-sectional view of the stress and the deformation on the chamber. The maximum deflection is around 100 µm, which occurs near the outlet of the top membrane. The higher deflection at the outlet area is attributed to the lack of support pillars; however, the 100 µm deflection should not

cause structural problems as the pillar height is 800 µm. In addition, the top membrane deflection near the outlet can be reduced by appropriately placing pillars or increasing the membrane thickness around the outlet. The latter was implemented in the actual fabrication process (see figure 7(b)(II)). Figure 5(b) represents the overall deflection characteristics of the top membrane indicating a fairly uniform deflection throughout the chamber area and it is around 60-80 µm, ~10% of the gap between the top and bottom membrane.

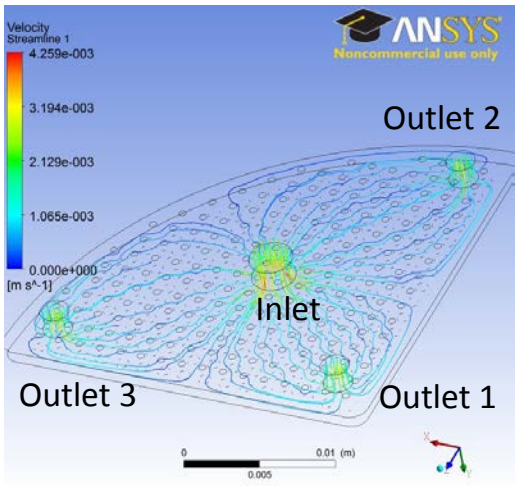

Figure 6: ANSYS simulation results on fluid flow of 1.0ml/min.

For the case of flushing the device or rapidly delivering medications, it is desirable to have both an inlet and outlet on the top of each quadrant. To encourage a uniform distribution of the pumped fluid velocity, each quadrant contained a single inlet and multiple outlets. A flow analysis using ANSYS was performed to determine if this design allowed for uniform flow through the device. As in the structural analysis case, only one quadrant was considered for this analysis. As an illustration, figure 6 shows the ANSYS computed streamlines for the flow through one quarter of the device. The flow paths indicate a fairly uniform flow characteristic throughout the chamber. To quantify the uniformity; two inlet flow rates were investigated to see their effect on the outlet flow rates. The results are given in Table 2. The flow mass injected from the inlet is conserved. For the flow of 1.0 ml/minute, the flow rate at outlet 1 is 13.57% and 13.25% higher than that of outlet 2 and 3, respectively. When the flow rate is increased to 5.0 ml/min, the difference of the flow rate of outlet 1 has decreased slightly to 12.83% and 12.29% higher than that of outlet 2 and 3, respectively. Better inlet and outlet placement can mitigate the flow rate differences; however, in this work no effort for further flow optimization was performed.

Table 2: ANSYS computed flow rates at inlet and outlet channels

Inlet (ml/min)	Outlet 1 (ml/min)	Outlet 2 (ml/min)	Outlet 3 (ml/min)
1.000	0.36186	0.31862	0.31952
5.000	1.768	1.567	1.573

3.2 Fabrication and Testing

3.2.1 Material Selection

RTV-4234-T4 silicone was selected over the widely used PDMS. Although some properties such as the biocompatibility and tensile strength (RTV-4234-T4: 6.7 MPa; PDMS: 7.1MPa) are similar for both materials (RTV-4234-T4 at 6.7 MPa; PDMS at 7.1MPa), the major consideration was given to elongation percentage and the tear strength. The elongation percentage of RTV-4234-T4 and PDMS are 400% and 120% respectively, while tear strength (Die B) is 150 ppi for RTV-4234-T4 and 5 ppi for PDMS [23, 25]. As pointed out in the introduction, high tear strength is critical for devices in direct contact with soft tissues, especially when used for implants and wound dressings requiring removal or regular replacement [17]. The high elongation property of RTV-4234-T4 is also very attractive because it measures flexibility, a key property which indicates the conformability of the material. In the cases of prosthetic implant or wound dressing applications, conformal contact of the device to the soft tissue is generally required.

In comparison to PDMS, the knowledge on RTV-4234-T4 silicone is very limited with regard to porosity, solvent/small molecule absorption, radiation hardness, and aging, so additional studies should be implemented. Preliminary investigations performed as a part of this study show there are no detectable changes to the material in ethanol (99.5%) or in a saline solution for extended amounts of time (>24 hours). UV exposure for 12 hours also does not seem to affect the material. These tests show the ability of the material to survive in common sterilization conditions; however more tests are needed in order to fully understand the potentials and limitations of RTV-4234-T4 for biomedical applications.

3.2.2 Molding

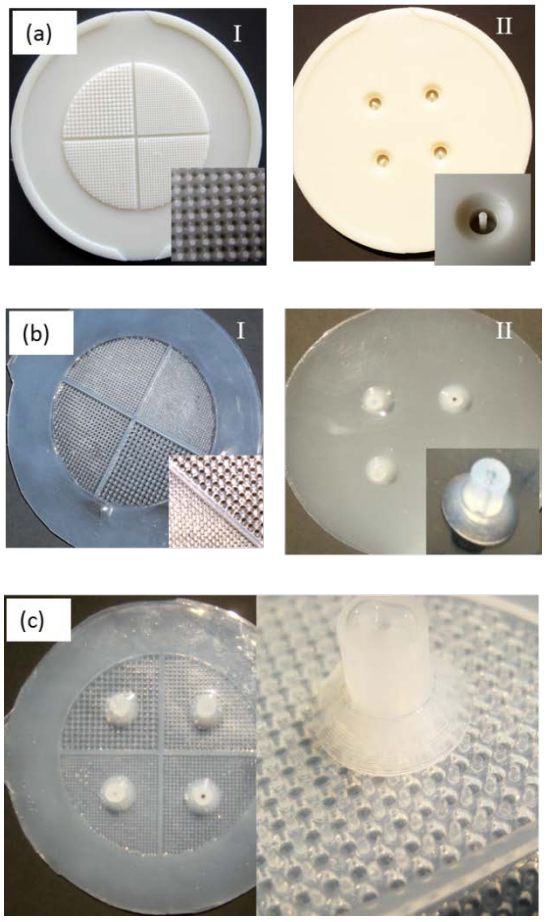

Figure 7: Various stages of two-layer fabrication process (a)(I) bottom mold, (a)(II) top mold, (b)(I) bottom membrane (b)(II) top membrane and (c) fabricated patch and its close-up .

Results at various stages of the two-layer fabrication process are depicted in figure 7. Process and material optimizations are needed at all stages of the fabrication. The mold material should be resilient to chemicals and withstand temperature conditions encountered during the curing process of the molded material. In this case, Accura 25 was selected over alternative resins for mold fabrication. The CTE (coefficient of thermal expansion) mismatch between the mold and the polymer is another factor that should be taken into consideration that directly affects the geometry of the micro features. In these experiments, no attempts have been made to understand the CTE mismatch characteristics of these materials. This is mainly due to non-availability of CTE data for RTV-4234-T4. To mitigate CTE mismatch effect, the low curing temperature is implemented.

Releasing the molded parts is another area that needs specific attention; microstructures should remain intact during the release, and a release agent should not interfere with subsequent bonding processes. Two different mold release coatings, nickel and parylene, were employed to facilitate the release of molded parts. No liquid based mold release agents were tried as they tend to interfere with bonding processes. In the case of the nickel coating, many of the pillars and the parts that extend deepest into the mold, appear to break; however, almost all the pillars were intact in the case of the *parylene coating. It was also found that a single parylene coating can last several molding runs, showing that parylene adheres well to the mold and does not interact with* RTV-4234-T4.

The flow of the molding material into the microscale features of the mold requires low viscosity molding materials. The typical value of the base material with curing agent for RTV-4234-T4 is 37000 cP, extremely high and not suitable for micromolding. As described in section 2.2, hexane was used for dilution of RTV-4234-T4 and the viscosity of the mixture was reduced to 95 cP. The viscosity was increased to 116 cP after adding the

curing agent and degassing process. This increase in viscosity from 95 to 116 cP is not significant enough to cause problems. It is however necessary that degassing time and conditions are kept the same in order to achieve repeatable results. Longer delay time between mixing and molding as well as temperature deviations can lead to viscosity variations, due to different degrees of partial curing. Furthermore, same vacuum conditions should be applied for degasing as variations in vacuum levels can result changes in hexane evaporation.

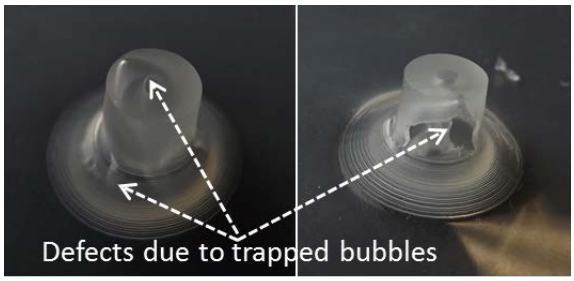

Figure 8: Trapped bubbles and the resulting defect on high aspect ratio trench molding

Even though the dilution of RTV-4234-T4 is necessary for this process, the presence of hexane in the silicone mixture complicates the curing process. First, it is difficult to cure the materials at room temperature. The accelerated curing at a higher temperature creates trapped air bubbles in the membranes caused by hexane entrapment due to evaporation. The optimized temperature for curing RTV-4234-T4 was determined to be 60°C for 30 minutes, providing enough time for the hexane to evaporate before the silicone hardens. Even at these conditions, bubble formation is particularly problematic if the mold has high aspect ratio trenches similar to 10 mm tubing connector shown in figure 8. In extreme cases, a two-step molding process is needed. First, trenches should be partially filled and cured before pouring in the remaining molding material and leveling the mold as described in the experimental section. It was observed that no disparities or fragility was noticeable between the two molding layers of RTV-4234-T4. Another factor to consider with the addition of hexane is shrinkage due hexane evaporation. In this design, the molded micro features are not affected; however, total membrane thickness shrinkage at this ratio is ~45%.

3.2.3 Bonding

The bond between membranes has to be mechanically strong and chemically stable to withstand operational conditions. Visual examination of the cross-section of the bonded membranes depicted a clean fuse, and the interface was marginally visible. Tests performed using the structure shown in figure 3 used to quantify delamination pressures, and it was found to be between 100 to 170 kPa, well above the typical 18 kPa used for NPWT. The positive pressure applied during fluid delivery is negligible. The variation of bond strength is typically caused by the difference in time delay between plasma activation and bonding. A longer delay causes free bond sites in the silicone to reorient before bonding, resulting in a variation in bond strength. This behavior has previously been reported in comparison studies performed for bonding of PDMS-PDMS using plasma and corona discharge activated surfaces [26].

The bond strength was also found not to be affected by extended exposure to ethanol and UV light, typical conditions encountered in the sterilization process. Only saline was used to mimic the biological conditions encountered during applications, and no changes to the bond strength were observed after exposure to the saline for 24 hours. Although the effect of biofilm formation and biological media is not yet known, these preliminary results indicate that these devices should withstand the operational and environmental conditions experienced during wound healing studies.

Plasma activated bonding can warrant its own compromises because applied pressure during bonding may exceed the structural tolerance of the device, resulting in the formation of bonding in undesired areas. This is particularly problematic when both layers of the device are made with a flexible substrate and larger cavity structures are present. In this particular process, COMSOL simulation was used to gauge the maximum deflection in the Z direction (along the pillars) and

was found to be 72 µm, less than 10% of the chamber height for the applied pressure of 20 kPa. Thus, the pillars could withstand the applied bonding pressure, and the structural integrity was uncompromised during the bonding process. Although the simulations performed here are specific to the given device, similar studies are needed to verify the viability of the fabrication method and conditions for other microfluidic devices. As microfluidic device fabrication is not governed by design rules due to lack of standards in materials and methodologies, the fabrication related issues in device functionality are mostly overlooked. Typically, solutions are sought after the problem is encountered. The results here highlight some of the issues that have to be taken into general consideration when fabricating compliant microfluidic devices.

3.2.4 Operation

Figure 9: Fabricated device attached to human forearm (no wound).

Figure 9 shows a picture of the fabricated device attached to a human hand (no wound) to show the intended application. The initial tests performed in laboratory conditions (see figure 4(a) and 4(b)) show that this patch is capable of delivering and extracting fluids as well as applying vacuum to the test patch, which mimics a wound bed. Experiments are scheduled to occur soon to confirm the applicability of the device for real-world wound-healing studies using porcine models.

4. **Conclusion:**

The design and fabrication of a compliant microfluidic device using a two-layer molding process has been demonstrated. With a bond strength exceeding 100 kPa, the device integrity during fabrication and operation has been verified using computational simulations and experimental laboratory tests. The device is capable of delivering and extracting fluid to and from a wound site. Although the effect of biofilm formation and biological media is not yet known, preliminary sterilization results indicate that a device made of RTV-4234-T4 should withstand an operational environment. Although the device is also designed to induce microdeformation to a wound bed with NPWT the effectiveness is yet to be quantified using animal models.

The fabrication process and results described are specific to the intended device type; however, this investigation highlights the important areas that need to be considered when fabricating microfluidic devices using compliant substrates. It also shows an alternative to PDMS microfluidic devices for clinical application. Other areas include usefulness of numerical simulations to verify fabrication aspects, design considerations for multilayer fabrication, and dilution of molding materials and its effect.

Acknowledgements:

The project is supported by a U.S. Army Medical Research Material Command (MRMC) Grant, funding opportunity W81XWH-11-1-0834. We appreciate the contributions from Prof. Harry Stephanou and Manoj Mittal from the University of Texas at Arlington Research Institute (UTARI); Col. Robert Hale (DDS), Dr. Kai Leung, and Dr. Rodney Chan (MD) from the US Army Dental and Trauma Research Detachment in San Antonio, Texas; Prof. Robert Galiano, Prof. Tom Mustoe, and Dr. Claudia Chavez, Division of Plastic Surgery at Northwestern University; and Dr. *Joseph Rosen (MD) and Sarah Long from Mayflower* Strategy Group, LLC.

References:

[1] Yeo L Y, Chang H -C, Chan P P Y and James R. Friend J R 2011 Microfluidic Devices for Bioapplications *small* **7 (1)** 12–48

[2] Gray B L 2012 *Proceedings of SPIE* **8344** 834419-(1-8)

[3] Tseng W-Y, J S Fisher J S, J L Prieto J L, Rinaldi K, Alapati G and Lee A P 2009 A slow-adapting microfluidic-based tactile sensor *J. Micromech. Microeng.* **19** 085002

[4] Kane BJ, Younan G, Helm D, Dastouri P, Prentice-Mott H, Irimia D, Chan RK, Toner M and Orgill DP. 2010 *J. Biomed. Mater. Res. A* **95(2)** 333-40

[5] Merchant Z H, Lo J F and Eddington D T 2011 *Journal of Undergraduate Research* **4** 16-20

[6] http://www.uta.edu/utamagazine/2011/02/biomask-2025/

[7] Whitesides G M and Stroock A D 2001 *Physics Today* **54 (6)** 42-48

[8] Van Midwoud P M, Janse A, Merema M T, Groothuis G M and Verpoorte E 2012 *Anal. Chem.* 84 **(9)** 3938–3944

[9] Ziegler D Suzuki T and Takeuchi S 2006 *J. Microelectromech. Syst.* **15(6)** 1477-1482

[10] Wan C R, Chung S and Kamm RD 2011 *Annals of Biomedical Engineering* **39 (6)** 1840–1847

[11] McDonald J C, Duffy D C, Anderson J R, Chiu D T, Wu H, Schueller O J and Whitesides G M 2000) Electrophoresis **21(1)** 27-40

[12] McDonald J C and Whitesides G M 2002 *Accounts of Chemical Research* **35(7)** 491-499.

[13] Kuncová-Kallio J and Kallio P J *2006 Conf. Proc. IEEE Eng. Med. Biol. Soc*. **1** 2486-2489

[14] Toepke M W and Beebe D J 2006 *Lab on a Chip* 6 1484-1486

[15] Chang W-J, Akin D, Sedlak M, Ladisch M R and Bashir R 2003 *Biomed. Microdev.* 5(4) 281-290

[16] Prakash A R, Adamia S, Sieben V, Pilarski P, Pilarski L M, and Backhouse C J 2006 *Sensors and Actuators B* 113(1) 398-409

[17] Aziz T, Waters M, Jagger R 2003 *Journal of Dentistry* 31 67–74

[18] Becker H and Gärtner C 2008 *Analytical & Bioanalytical Chemistry* **390(1)** 89-111

[19] Choi C J and Cunningham B T *2006 Lab on a Chip* **6** 1373-1380

[20] Kuo J S, Ng L, Yen G S, Lorenz R M, Schiro P G, Scott Edgar J, Zhao Y, Lim D S W, Allen P B, Jeffries G D M and Chiu D T *2009 Lab on a Chip* **9** 870-876

[21] Blake A J, Pearce T M, Rao N S, Johnson S M and Williams JC 2007 *Lab on a Chip* **7** 842–849

[22] Garst S, Schuenemanna M, Solomona M, Atkinb M and Harveyac E *2005 Proceedings of 55th Electronic Components and Technology Conference* **1** 603 – 610

[23] https://www.xiameter.com

[24] Saxena V, Hwang C W, Huang S, Eichbaum Q, Ingber D, Orgill D P. 2004 *Plast. Reconstr. Surg.* **114** 1086–1096; 086-96; discussion 1097-1098

[25] http://www.dowcorning.com

[26] Eddings M A, Johnson M A and Gale B K 2008 J. Micromech. Microeng. **18** 067001

APPENDIX 2:

All personnel receiving pay from research effort are employees of the University of Texas at Arlington Research Institute.

1. Eileen Moss Clements, Director of Research

2. Manoj Mittal, Research Scientist II

3. Muthu Wijesundara, Principal Research Scientist

4. Raminderdeep Sidhu, Research Scientist I

5. Jeongsik Shin, Senior Research Scientist

6. Kyle Shook, UTA Graduate Student

7. Sean Collignon, Research Scientist I

8. Corwin Lester, Research Scientist